JACS
JOURNAL OF THE AMERICAN CHEMICAL SOCIETY
pubs.acs.org/JACS

Article

Stereocontrolled Self-Assembly of a Helicate-Bridged $Cu^{I}_{12}L_4$ Cage That Emits Circularly Polarized Light

Huangtianzhi Zhu, Luca Pesce, Rituparno Chowdhury, Weichao Xue, Kai Wu, Tanya K. Ronson, Richard H. Friend,* Giovanni M. Pavan,* and Jonathan R. Nitschke*

Cite This: J. Am. Chem. Soc. 2024, 146, 2379−2386

Read Online

ACCESS | Metrics & More | Article Recommendations | Supporting Information

ABSTRACT: Control over the stereochemistry of metal−organic cages can give rise to useful functions that are entwined with chirality, such as stereoselective guest binding and chiroptical applications. Here, we report a chiral $Cu^{I}_{12}L_4$ pseudo-octahedral cage that self-assembled from condensation of triaminotriptycene, aminoquinaldine, and diformylpyridine subcomponents around Cu^{I} templates. The corners of this cage consist of six head-to-tail dicopper(I) helicates whose helical chirality can be controlled by the addition of enantiopure 1,1′-bi-2-naphthol (BINOL) during the assembly process. Chiroptical and nuclear magnetic resonance (NMR) studies elucidated the process and mechanism of stereochemical information transfer from BINOL to the cage during the assembly process. Initially formed $Cu^{I}(BINOL)_2$ thus underwent stereoselective ligand exchange during the formation of the chiral helicate corners of the cage, which determined the overall cage stereochemistry. The resulting dicopper(I) helicate corners of the cage were also shown to generate circularly polarized luminescence.

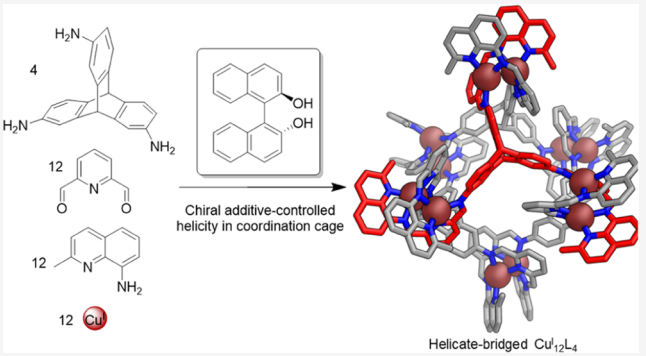

INTRODUCTION

The stereochemical configurations of biomolecules are crucial to the recognition processes that underpin their functions, such as the stereoselective interactions between enzymes and their substrates, and the folding of proteins and nucleic acids into functional higher-order structures.[1−3] These processes have inspired the design of artificial supramolecular systems where chirality is integral to function, such as metal−organic cages.[4−13] Enantiopure metal−organic cages enable applications in the fields of chiral recognition, separation, catalysis, and chiroptics,[14−21] thus extending the functions of achiral and racemic coordination cages.[22−27] For example, work from the Raymond and Bergmand groups reported an enantiopure $[Ga^{III}_4L_6]^{12-}$ tetrahedron capable of dynamically resolving racemic ruthenium complexes.[28] More recently, circularly polarized luminescence (CPL)-active metal−organic assemblies,[29−31] which hold great potential for chiroptical devices and display technologies, have been reported by the Sun[32] and Clever[33] groups. The chirality of those cages frequently originates from the Δ vs Λ handedness of metal vertices, as well as stereocenters incorporated into ligands.[34−39] We thus anticipated that the incorporation of new chiral moieties, such as chiral Cu^{I} helicates,[40,41] into cage frameworks could enable the exploration of new functions linked to stereochemistry.[42,43]

Helical supramolecular structures can be prepared by the coordination-driven self-assembly of multitopic ligands around different metal ions. These structures have enabled different functions.[44−48] Methods to influence the stereochemistry of these assemblies have focused principally upon the use of ligands containing asymmetric centers, with a few notable exceptions, in which chiral information transfers from a guest or solvent to the assembly.[49−58]

A complementary, and rarely employed, strategy involves the use of chiral chelating additives that bind metal ions weakly prior to assembly,[59] followed by ligand exchange to define the stereochemistry of complexes that incorporate more robustly coordinating ligands. This strategy requires finely tuned binding affinities to secure stereocontrol. Complexation of a chiral additive that binds too strongly renders subsequent ligand exchange infeasible, whereas an additive that binds too weakly is unlikely to affect stereocontrol.

Here, we report the self-assembly of a $Cu^{I}_{12}L_4$ cage **1**, the corners of which are composed of dicopper(I) helicates. Prior work has shown that both head-to-tail (HT) and head-to-head (HH) dicopper(I) helicates formed during the subcomponent

Received: October 12, 2023
Revised: December 20, 2023
Accepted: December 23, 2023
Published: January 22, 2024

https://doi.org/10.1021/jacs.3c11321
J. Am. Chem. Soc. 2024, 146, 2379−2386

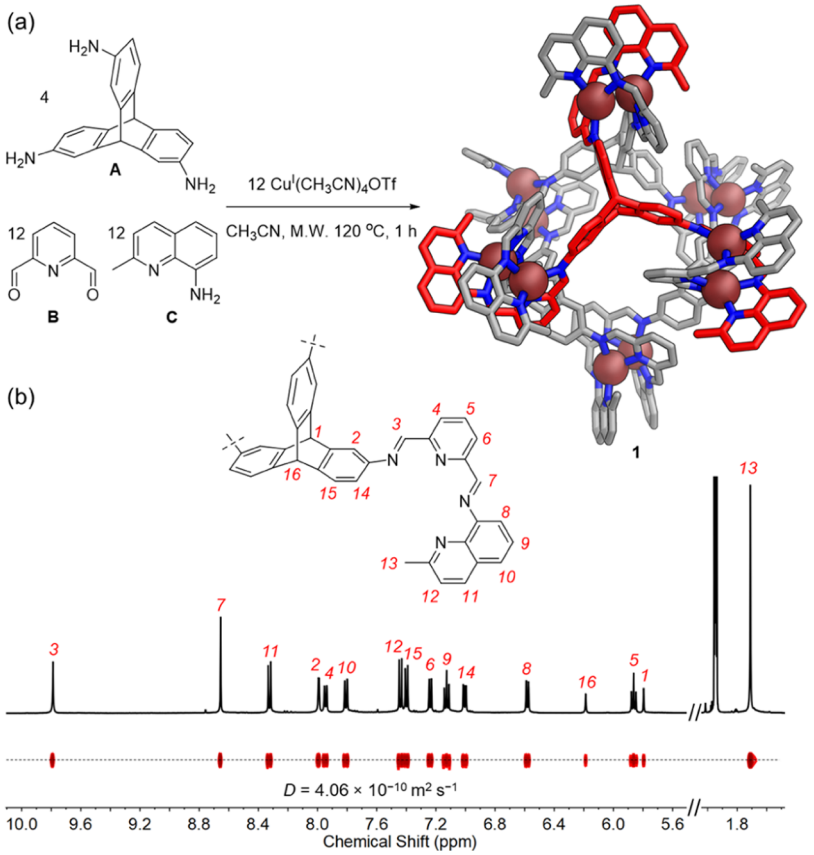

Figure 1. (a) Subcomponent self-assembly of pseudo-octahedral cage **1** with the cage shown as its DFT model. Carbon is shown in gray, nitrogen atoms are blue, copper(I) atoms are burgundy. The carbon atoms of one ligand are shown in red for clarity. (b) Partial chemical structure of the ligand showing NMR peak assignments and ^{1}H NMR and DOSY spectra (400 MHz, 298 K, CD_3CN) of **1**, showing assignments.

self-assembly of systems that contain anilines with 2,6-diformylpyridine and 8-aminoquinolines.[60] In this study, the use of the tris(aniline) 2,7,14-triaminotriptycene **A** (Figure 1) in such systems was found to drive the formation of HT helicates, which formed the six corners of a *T*-symmetric $Cu^{I}_{12}L_4$ pseudo-octahedral cage.

Cage **1** exhibited stereochemical information transfer, whereby the stereochemistry of its helicate corners was governed by the initial binding of 1,1′-bi-2-naphthol (BINOL) to Cu^{I}. This weak binding resulted in the formation of a chiral intermediate, which then underwent stereoselective ligand exchange during the formation of the helicate corners of **1** to form cages with exclusively *P* or *M* corner stereoconfigurations. Once formed stereoselectively, **1** did not racemize upon heating to 353 K for 15 days in the absence of BINOL.

Cu^{I} assemblies have potential applications based on their electronic and photophysical features.[61−63] Following its stereoselective preparation, we found that **1** emitted CPL, potentially enabling its use in the many applications underpinned by circularly polarized luminescence.[29−33]

RESULTS AND DISCUSSION

The reaction of 2,7,14-triaminotriptycene (**A**, 4 equiv), 2,6-diformylpyridine (**B**, 12 equiv), 8-aminoquinaldine (**C**, 12 equiv), and $Cu^{I}(CH_3CN)_4OTf$ (12 equiv) produced cage **1** as the uniquely observed product (Figure 1a). Electrospray ionization mass spectrometry (ESI-MS) indicated a $Cu^{I}_{12}L_4$ formulation (Figure S8), allowing us to infer that **1** consists of four triptycene moieties and six dicopper(I) helicates. The ^{1}H NMR spectrum of **1** contained 16 signals (Figure 1b), with all signals displaying the same diffusion coefficient in the ^{1}H diffusion-ordered spectroscopy (DOSY) spectrum. Two-dimensional NMR spectra allowed the assignment of each proton signal of **1** (Figures S4−S7).

The presence of only one set of ligand protons indicated a high-symmetry configuration for **1**, in which all six helicates adopt the same HT or HH conformation. Identical results were also obtained using Cu^{I} salts with different anions, indicating that anions did not exercise a templating effect during cage formation (Figures S10−S16).[64−67] Changing 8-aminoquinaldine to 8-aminoquinoline, or using 4-bromo-2,6-diformylpyridine in place of the nonbrominated analogue, yielded products with the same $Cu^{I}_{12}L_4$ framework (Figures S17−S20). Following work undertaken by Mastalerz,[8] we infer the curvature of **A** to have been essential to the formation of **1**, as planar triamines did not generate discrete products (Figure S21).

Despite more than 600 individual attempts to grow single crystals of **1**, none of the crystals obtained diffracted strongly enough to obtain a crystal structure. Density functional theory (DFT) calculations were thus carried out to elucidate the structure of **1**. Different configurations of four triptycene units and six dicopper(I) helicates were combined to form discrete structures. Two conformations of triptycene, denoted "inward" and "outward", and two helicate configurations, head-to-head and head-to-tail, were considered during structural optimiza-

https://doi.org/10.1021/jacs.3c11321
J. Am. Chem. Soc. 2024, 146, 2379−2386

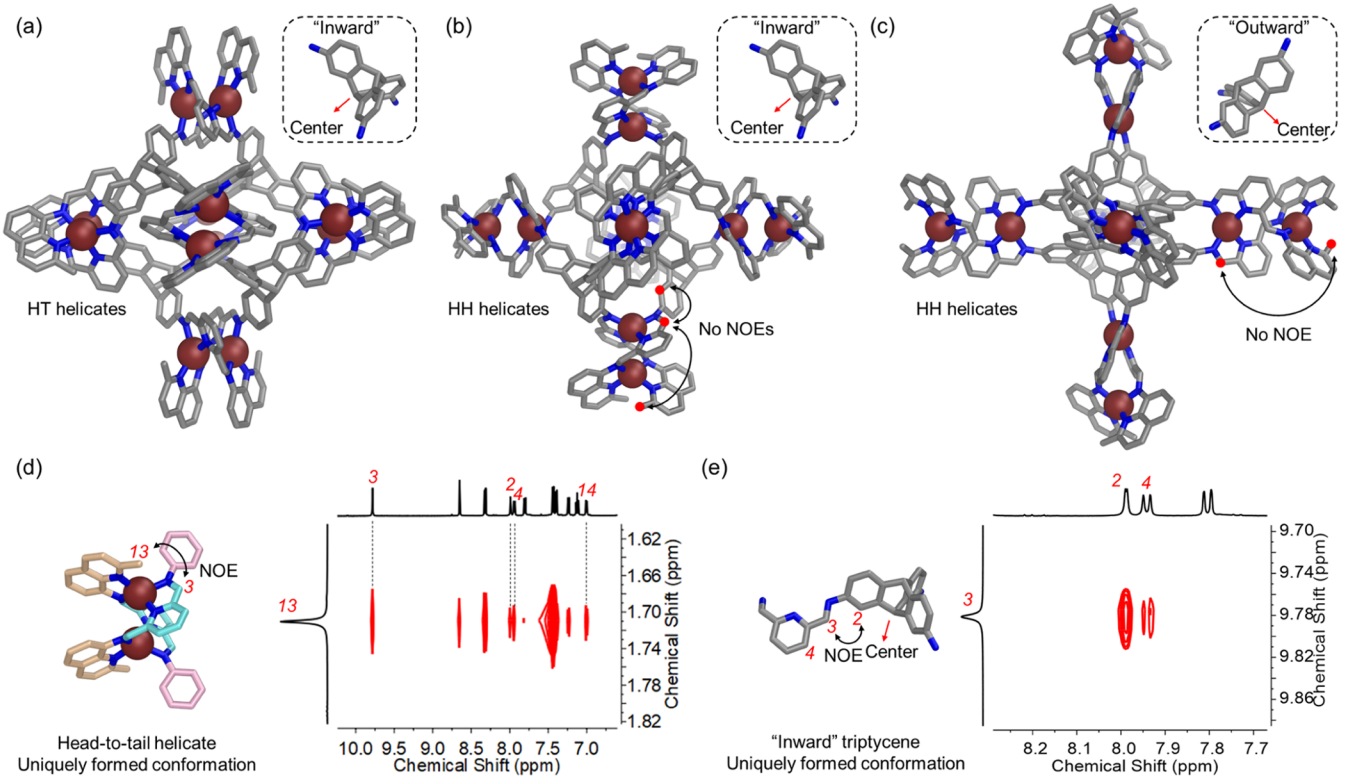

Figure 2. DFT-optimized structures of **1** with (a) "inward"-facing triptycenes and HT helicates, (b) "inward"-facing triptycenes and HH helicates, and (c) "outward"-facing triptycenes and HH helicates. (d, e) Partial NOESY spectra (400 MHz, 298 K, CD_3CN) of **1** that support the HT conformation and "inward"-facing triptycene configuration, supporting the assignment to **1** of the configuration shown in (a).

tions. Full details of the structural optimizations undertaken are given in Section 7 in the Supporting Information.

Figure 2a–c shows three of the lowest-energy *T*-symmetric frameworks for **1**, each of which is consistent with the ESI-MS and one-dimensional ^{1}H NMR data obtained. Only the structure shown in Figure 2a matches with all of our 2D NMR data in two key ways. First, as shown in Figure 2d, nuclear Overhauser effect (NOE) magnetization transfer is observed between methyl proton H_{13} and imine proton H_3. This observation is consistent with a head-to-tail helicate configuration but not a head-to-head one. Second, the NOE correlation shown in Figure 2e between imine proton H_3 and triptycene proton H_2 is consistent with the "inward" triptycene conformation shown, but not an "outward" one. We thus infer **1** to adopt the structure shown in Figure 2a, whose $Cu^I\cdots Cu^I$ distances also match more closely those of dicopper(I) helicates reported than do the other structures considered.[60,68] The fourth structure, containing head-to-tail helicates and "outward"-facing triptycenes, was eliminated on account of steric hindrance, as shown in Section 7 in the Supporting Information.

The cavity of the conformation of cage **1** shown in Figure 1a has a volume of 344 Å^3, calculated using MoloVol (Figure S22).[69] We were not able to observe neutral guest binding within this cavity, however (Figures 3 and S32). We inferred this lack of binding to be due to large peripheral pores and the lack of stacking interactions between the host and potential guests. To probe the binding ability of the cage toward anionic guests,[70,71] **1** was treated with anions that included organic sulfonates and tetraphenylborate, all of which were complexed by **1** in fast exchange on the NMR time scale. Cage **1** bound 1-hexylsulfonate with a binding constant >10^3 M^{-1}, whereas its

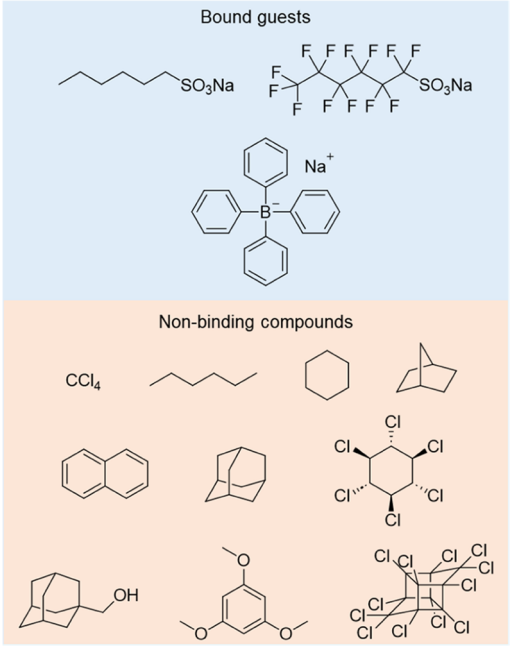

Figure 3. Prospective guests were tested for binding within **1**.

complexation of perfluoro-1-hexanesulfonate, a chronic pollutant that has attracted interest due to the need for its environmental remediation,[72] was weaker, which we attribute to the electron-deficient character of the guest perfluoroalkane chain (Figures S23–S28). We infer that these two guests thread into the cavity of the cage, as reflected in downfield shifts of triptycene imine H_3 and pyridine proton H_4, and an

https://doi.org/10.1021/jacs.3c11321
J. Am. Chem. Soc. 2024, 146, 2379–2386

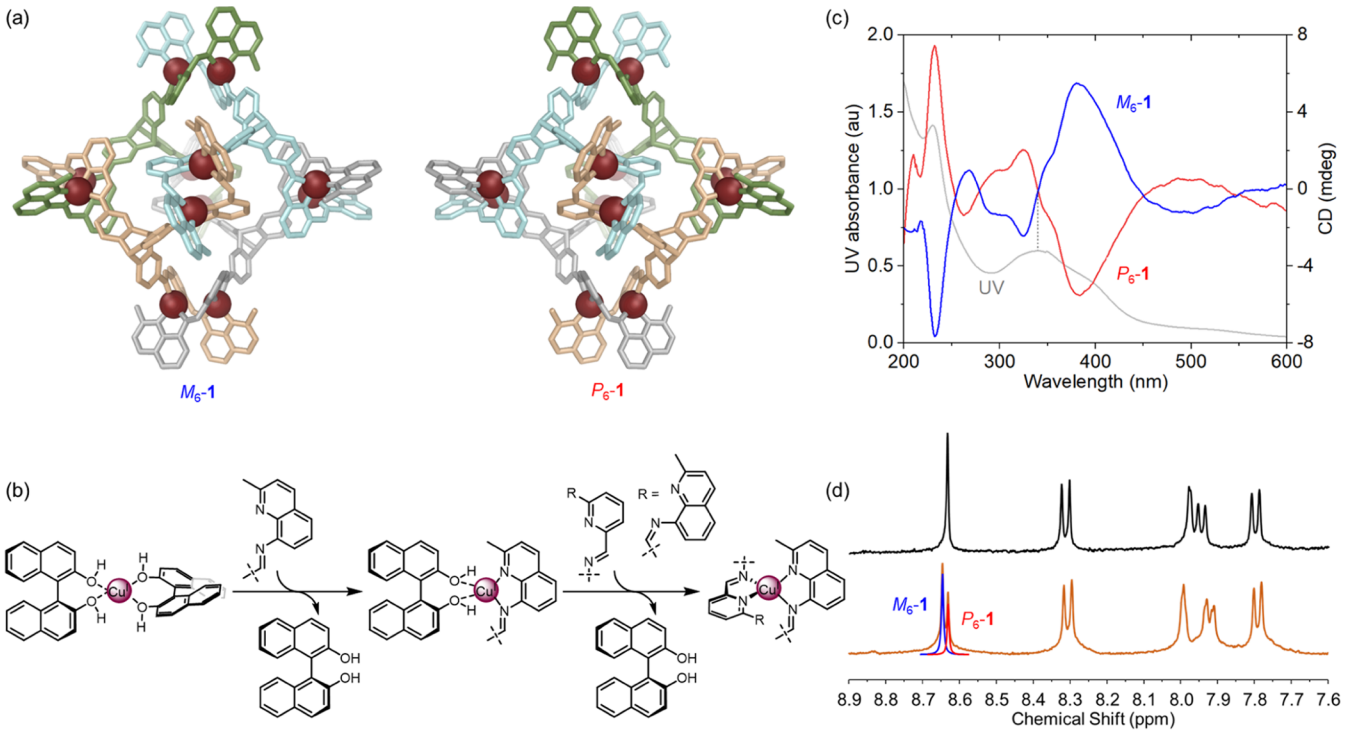

Figure 4. (a) Enantiomers of **1**. Ligands are individually colored to show the helicity. (b) Proposed mechanism of stereoinduction during the formation of the Cu^I stereocenters of **1**. (c) UV−Vis and CD spectra of M_6- and P_6-biased **1** in acetonitrile. (d) ^{1}H NMR spectra (400 MHz, 298 K, CD_3CN) of M_6-biased **1** before (top, black) and after (bottom, orange) the addition of 2 equiv of Δ-TRISPHAT.

upfield shift of pyridine proton H_5. The bulky anion tetraphenylborate interacted weakly with **1** at its peripheral openings, as evidenced by upfield shifts of the pyridine H_5 and imine H_7 proton signals (Figures S29 and S30).

Cage **1** is formed as a racemic mixture, where the corners of each cage consist of either six *M*-helicates or six *P*-helicates (denoted as M_6-**1** and P_6-**1**, respectively, Figure 4a), as reflected in a featureless circular dichroism (CD) spectrum. We envisaged that **1** might be formed stereoselectively through the addition of a chiral auxiliary.[73] Screening prospective auxiliaries revealed that the presence of enantiopure 1,1′-bi-2-naphthol (BINOL) during the self-assembly of **1** led to stereocontrol (Scheme S3). After removal of the BINOL by washing with ethyl acetate and diethyl ether, cage **1** displayed clear CD Cotton effects from 350 to 450 nm, consistent with chiral induction during its synthesis. Specifically, the use of (*S*)-BINOL (50 equiv) led to a higher population of P_6-**1**, as reflected in a negative Cotton effect at the MLCT band around 400 nm,[69] whereas (*R*)-BINOL (50 equiv) favored the formation of M_6-**1**, with a mirror-image CD spectrum (Figure 4c). Although BINOL-derived ligands have been employed as building blocks in chiral cages,[74,75] the use of BINOL as a chiral additive has been less explored.[76]

The enantiomeric excess (*ee*) of **1** prepared in the presence of BINOL was determined by deconvolution and integration of the ^{1}H NMR spectra containing tetrabutylammonium Δ-tris(tetrachlorocatecholato)phosphate (Δ-TRISPHAT) as a chiral discrimination agent.[77−79] The imine signal H_{13}, originally a singlet, split in two upon the addition of 2 equiv of Δ-TRISPHAT (Figure 4d). NMR integration indicated an *ee* of 29% was obtained following the use of 100 equiv of BINOL. The intensity of the CD signals did not decrease after the sample was heated to 80 °C for 15 days, indicating a strong chiral memory effect owing to the cooperative locking together of the structure by 48 N → Cu^I coordinative bonds (Figure S33).[80]

The effects of BINOL upon the stereoinduction of **1** were further probed by a series of self-assembly experiments (Figures S33−S40). Three parallel reactions were performed, each containing different amounts of (*R*)-BINOL. The intensity of the CD signal at 385 nm was found to correlate positively with the amount of (*R*)-BINOL added. We fitted these data using 1:1 and 1:2 binding models (Figure S36). A 1:2 binding mode provided a better fit and gave a maximum CD intensity at 385 nm of 10.6 mdeg. The *ee* value obtained from NMR integration was also plotted against the amount of (*R*)-BINOL added, and the relationship was also analyzed using the same 1:2 model (Figure S39). The CD intensity at 385 nm was found to correlate linearly with the NMR-determined *ee* of **1** (Figure S40).

The mechanism of chiral induction was probed through a series of control experiments. A racemic sample of **1** was mixed with 50 equiv of (*R*)-BINOL in acetonitrile and heated to 343 K over 36 h. The ratio of M_6-**1** to P_6-**1**, measured by NMR integration, did not change (Figure S41). Heating (*R*)-BINOL with P_6-**1**, or (*S*)-BINOL with M_6-**1**, did not result in a reversal or decrease of the corresponding CD signal, indicating that helical handedness was imprinted by BINOL during the formation of the cage and that the chiral memory effect was impervious to BINOL thereafter. Moreover, the treatment of **1** with BINOL did not cause any NMR chemical shift changes, indicating that host−guest interactions did not occur between **1** and BINOL (Figure S42).

We thus infer that (*S*)- or (*R*)-BINOL coordinates to Cu^I initially, yielding a chiral intermediate that undergoes further ligand exchange to stereoselectively produce the helicate

https://doi.org/10.1021/jacs.3c11321
J. Am. Chem. Soc. 2024, 146, 2379−2386

corners of the chiral cage framework (Figure 4b). Evidence of complexation between BINOL and Cu^{I} was observed by ^{1}H NMR (Figure S43). The nonlinear relationship between CD intensity and *ee* plotted against BINOL concentration (Figures S33−S38) also supports the formation of a $Cu^{I}(BINOL)_2$ complex, as noted above. Temperature-dependent *ee* and CD results (Figures S44 and S45) provide further support for our putative mechanism, as the weakly bound intermediate BINOL-Cu^{I} complexes would decomplex at higher temperatures, favoring cage formation pathways that do not implicate BINOL.

Stereocontrol during the synthesis of **1** was attempted through the addition of other chiral compounds that contain O, N, or P donor groups, and which may thus serve as bidentate or monodentate ligands to Cu^{I} (Figure S46). In all cases, either no stereoselectivity was observed or **1** was not formed (Figures S47 and S48). We thus conclude that BINOL operates in a "sweet spot", not binding so strongly to Cu^{I} that cage formation is inhibited but binding strongly enough to bias helical handedness.

We hypothesized that stereoselectively prepared **1** would emit circularly polarized light, as the MLCT states of copper(I) diimine complexes are known to be emissive.[81] A solution of **1** in acetonitrile was observed to luminesce following laser excitation at 400 nm, with an absolute quantum yield (QY) of 30% (Figure 5a). The steady-state photoluminescence (PL)

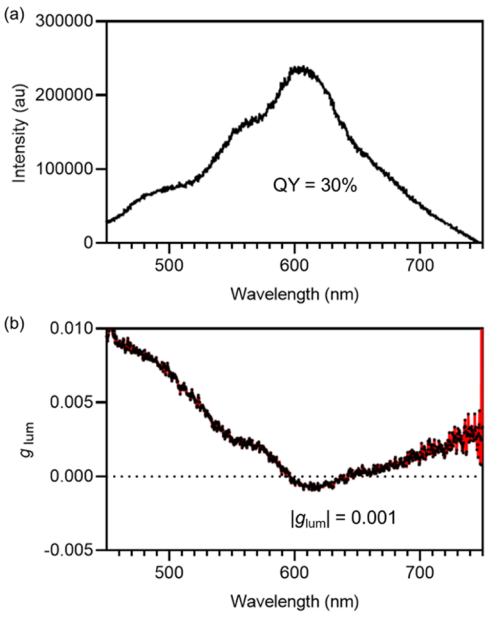

Figure 5. (a) PL spectrum of **1** in acetonitrile, at an excitation wavelength of 400 nm and a concentration of 10^{-5} M. (b) Determination of the $|g_{lum}|$ of **1** in acetonitrile.

spectrum revealed a broad emission from 400 to 750 nm, centered at 610 nm. Time-resolved PL analysis confirmed that the emission faded rapidly over the nanosecond time scale, precluding the presence of triplet-state-involved radiative decay. CPL measurements revealed that the helicity in **1** exhibited a dissymmetry factor ($|g_{lum}|$) of 0.001 (Figure 5b). While the lack of f electrons endows the cage with only a moderate $|g_{lum}|$, our results demonstrate the embedding of dicopper(I) helicate moieties within a cage framework to be effective for the fabrication of novel structures for CPL.

CONCLUSIONS

The formation of cage **1** thus validates a strategy of integrative self-sorting during the subcomponent self-assembly of complex structures, as each equivalent of symmetrical dialdehyde **B** must react with one **A** and one **C** to form the helicate corners. This strategy may also be extended to the preparation of larger cages that combine multiple subcomponents, for example, incorporating tetratopic or pentatopic amines with nonplanar cores. The six helicate corner structures also cooperatively increase the stability of **1**, as evidenced by its stereochemical memory effect, which should benefit its potential applications in other solvents, potentially including water, for stereoselective binding. Moreover, the method of stereoselective synthesis through the use of BINOL demonstrates a new mode of transferring stereochemical information from the environment during cage synthesis, potentially avoiding tedious covalent modifications of ligands with chiral substituents.

ASSOCIATED CONTENT

Data Availability Statement

Computational structures and outputs are available at 10.5281/zenodo.10372347.

Supporting Information

The Supporting Information is available free of charge at https://pubs.acs.org/doi/10.1021/jacs.3c11321.

Experimental procedures, NMR spectra, photophysical results, and computational details (PDF)

AUTHOR INFORMATION

Corresponding Authors

Richard H. Friend − *Cavendish Laboratory, University of Cambridge, Cambridge CB3 0HE, United Kingdom;* orcid.org/0000-0001-6565-6308; Email: rhf10@cam.ac.uk

Giovanni M. Pavan − *Department of Innovative Technologies, University of Applied Sciences and Arts of Southern Switzerland, CH-6962 Lugano-Viganello, Switzerland; Department of Applied Science and Techology, Politecnico di Torino, 10129 Torino, Italy;* orcid.org/0000-0002-3473-8471; Email: giovanni.pavan@polito.it

Jonathan R. Nitschke − *Yusuf Hamied Department of Chemistry, University of Cambridge, Cambridge CB2 1EW, United Kingdom;* orcid.org/0000-0002-4060-5122; Email: jrn34@cam.ac.uk

Authors

Huangtianzhi Zhu − *Yusuf Hamied Department of Chemistry, University of Cambridge, Cambridge CB2 1EW, United Kingdom*

Luca Pesce − *Department of Innovative Technologies, University of Applied Sciences and Arts of Southern Switzerland, CH-6962 Lugano-Viganello, Switzerland;* orcid.org/0000-0001-6364-9577

Rituparno Chowdhury − *Cavendish Laboratory, University of Cambridge, Cambridge CB3 0HE, United Kingdom*

Weichao Xue − *Yusuf Hamied Department of Chemistry, University of Cambridge, Cambridge CB2 1EW, United Kingdom*

Kai Wu − *Yusuf Hamied Department of Chemistry, University of Cambridge, Cambridge CB2 1EW, United Kingdom;* orcid.org/0000-0001-6336-7836

https://doi.org/10.1021/jacs.3c11321
J. Am. Chem. Soc. 2024, 146, 2379−2386

Tanya K. Ronson − *Yusuf Hamied Department of Chemistry, University of Cambridge, Cambridge CB2 1EW, United Kingdom;* orcid.org/0000-0002-6917-3685

Complete contact information is available at: https://pubs.acs.org/10.1021/jacs.3c11321

Notes

The authors declare no competing financial interest.

■ ACKNOWLEDGMENTS

This work was supported by the Engineering and Physical Sciences Research Council (EPSRC, EP/P027067/1) and the European Research Council (695009). G.M.P. acknowledges funding received from the European Research Council (818776). G.M.P. and L.P. also acknowledge the computational resources provided by the Swiss National Supercomputing Center. R.C and R.H.F. acknowledge funding from the European Union's Horizon 2020 research and innovation programme under the Marie Skłodowska-Curie grant agreements No. 859752 (HEL4CHIROLED)

■ REFERENCES

(1) Bentley, R. Role of sulfur chirality in the chemical processes of biology. *Chem. Soc. Rev.* **2005**, *34*, 609−624.
(2) Caner, H.; Groner, E.; Levy, L.; Agranat, I. Trends in the development of chiral drugs. *Drug Discovery Today* **2004**, *9*, 105−110.
(3) Yang, H.; Metera, K. L.; Sleiman, H. F. DNA modified with metal complexes: Applications in the construction of higher order metal−DNA nanostructures. *Coord. Chem. Rev.* **2010**, *254*, 2403−2415.
(4) Liu, M.; Zhang, L.; Wang, T. Supramolecular Chirality in Self-Assembled Systems. *Chem. Rev.* **2015**, *115*, 7304−7397.
(5) Ozores, H. L.; Amorín, M.; Granja, J. R. Self-Assembling Molecular Capsules Based on α,γ-Cyclic Peptides. *J. Am. Chem. Soc.* **2017**, *139*, 776−784.
(6) Sato, S.; Yoshii, A.; Takahashi, S.; Furumi, S.; Takeuchi, M.; Isobe, H. Chiral intertwined spirals and magnetic transition dipole moments dictated by cylinder helicity. *Proc. Natl. Acad. Sci. U.S.A.* **2017**, *114*, 13097−13101.
(7) Chen, L.-J.; Yang, H.-B.; Shionoya, M. Chiral metallosupramolecular architectures. *Chem. Soc. Rev.* **2017**, *46*, 2555−2576.
(8) Wagner, P.; Rominger, F.; Zhang, W.-S.; Gross, J. H.; Elbert, S. M.; Schröder, R. R.; Mastalerz, M. Chiral Self-sorting of Giant Cubic [8 + 12] Salicylimine Cage Compounds. *Angew. Chem., Int. Ed.* **2021**, *60*, 8896−8904.
(9) Maayan, G.; Ward, M. D.; Kirshenbaum, K. Folded biomimetic oligomers for enantioselective catalysis. *Proc. Natl. Acad. Sci. U.S.A.* **2009**, *106*, 13679−13684.
(10) Mishra, S. S.; Kompella, S. V. K.; Krishnaswamy, S.; Balasubramanian, S.; Chand, D. K. Low-Symmetry Self-Assembled Coordination Complexes with Exclusive Diastereoselectivity: Experimental and Computational Studies. *Inorg. Chem.* **2020**, *59*, 12884−12894.
(11) Zhu, C.; Tang, H.; Yang, K.; Fang, Y.; Wang, K.-Y.; Xiao, Z.; Wu, X.; Li, Y.; Powell, J. A.; Zhou, H.-C. Homochiral dodecanuclear lanthanide "cage in cage" for enantioselective separation. *J. Am. Chem. Soc.* **2021**, *143*, 12560−12566.
(12) Gidron, O.; Ebert, M.-O.; Trapp, N.; Diederich, F. Chiroptical Detection of Nonchromophoric, Achiral Guests by Enantiopure Alleno-Acetylenic Helicages. *Angew. Chem., Int. Ed.* **2014**, *53*, 13614−13618.
(13) Pan, M.; Wu, K.; Zhang, J.-H.; Su, C.-Y. Chiral metal−organic cages/containers (MOCs): From structural and stereochemical design to applications. *Coord. Chem. Rev.* **2019**, *378*, 333−349.
(14) Luo, D.; Wang, X.-Z.; Yang, C.; Zhou, X.-P.; Li, D. Self-Assembly of Chiral Metal−Organic Tetartoid. *J. Am. Chem. Soc.* **2018**, *140*, 118−121.
(15) Li, K.; Wu, K.; Fan, Y.-Z.; Guo, J.; Lu, Y.-L.; Wang, Y.-F.; Maurin, G.; Su, C.-Y. Acidic open-cage solution containing basic cage-confined nanospaces for multipurpose catalysis. *Natl. Sci. Rev.* **2022**, *9*, No. nwab155, DOI: 10.1093/nsr/nwab155.
(16) Han, Y.-F.; Jia, W.-G.; Yu, W.-B.; Jin, G.-X. Stepwise formation of organometallic macrocycles, prisms and boxes from Ir, Rh and Ru-based half-sandwich units. *Chem. Soc. Rev.* **2009**, *38*, 3419−3434.
(17) Howlader, P.; Zangrando, E.; Mukherjee, P. S. Self-Assembly of Enantiopure Pd_{12} Tetrahedral Homochiral Nanocages with Tetrazole Linkers and Chiral Recognition. *J. Am. Chem. Soc.* **2020**, *142*, 9070−9078.
(18) Seo, J. S.; Whang, D.; Lee, H.; Jun, S. I.; Oh, J.; Jeon, Y. J.; Kim, K. A homochiral metal−organic porous material for enantioselective separation and catalysis. *Nature* **2000**, *404*, 982−986.
(19) Zhou, Y.; Li, H.; Zhu, T.; Gao, T.; Yan, P. A Highly Luminescent Chiral Tetrahedral $Eu_4L_4(L')_4$ Cage: Chirality Induction, Chirality Memory, and Circularly Polarized Luminescence. *J. Am. Chem. Soc.* **2019**, *141*, 19634−19643.
(20) Lu, Z.; Ronson, T. K.; Heard, A. W.; Feldmann, S.; Vanthuyne, N.; Martinez, A.; Nitschke, J. R. Enantioselective fullerene functionalization through stereochemical information transfer from a self-assembled cage. *Nat. Chem.* **2023**, *15*, 405−412.
(21) Gadzikwa, T.; Bellini, R.; Dekker, H. L.; Reek, J. N. H. Self-Assembly of a Confined Rhodium Catalyst for Asymmetric Hydroformylation of Unfunctionalized Internal Alkenes. *J. Am. Chem. Soc.* **2012**, *134*, 2860−2863.
(22) Preston, D.; Lewis, J. E. M.; Crowley, J. D. Multicavity $[Pd_nL_4]^{2n+}$ Cages with Controlled Segregated Binding of Different Guests. *J. Am. Chem. Soc.* **2017**, *139*, 2379−2386.
(23) Ubasart, E.; Borodin, O.; Fuertes-Espinosa, C.; Xu, Y.; García-Simón, C.; Gómez, L.; Juanhuix, J.; Gándara, F.; Imaz, I.; Maspoch, D.; et al. A three-shell supramolecular complex enables the symmetry-mismatched chemo- and regioselective bis-functionalization of C_{60}. *Nat. Chem.* **2021**, *13*, 420−427.
(24) Borsley, S.; Haugland, M. M.; Oldknow, S.; Cooper, J. A.; Burke, M. J.; Scott, A.; Grantham, W.; Vallejo, J.; Brechin, E. K.; Lusby, P. J.; Cockroft, S. L. Electrostatic Forces in Field-Perturbed Equilibria: Nanopore Analysis of Cage Complexes. *Chem* **2019**, *5*, 1275−1292.
(25) Li, Y.; An, Y.-Y.; Fan, J.-Z.; Liu, X.-X.; Li, X.; Hahn, F. E.; Wang, Y.-Y.; Han, Y.-F. Strategy for the Construction of Diverse Poly-NHC-Derived Assemblies and Their Photoinduced Transformations. *Angew. Chem., Int. Ed.* **2020**, *59*, 10073−10080.
(26) Alimi, L. O.; Alyami, M. Z.; Chand, S.; Baslyman, W.; Khashab, N. M. Coordination-based self-assembled capsules (SACs) for protein, CRISPR−Cas9, DNA and RNA delivery. *Chem. Sci.* **2021**, *12*, 2329−2344.
(27) Wang, Z. J.; Clary, K. N.; Bergman, R. G.; Raymond, K. N.; Toste, F. D. A supramolecular approach to combining enzymatic and transition metal catalysis. *Nat. Chem.* **2013**, *5*, 100−103.
(28) Fiedler, D.; Leung, D. H.; Bergman, R. G.; Raymond, K. N. Enantioselective Guest Binding and Dynamic Resolution of Cationic Ruthenium Complexes by a Chiral Metal−Ligand Assembly. *J. Am. Chem. Soc.* **2004**, *126*, 3674−3675.
(29) Li, B.; Li, Y.; Chan, M. H.-Y.; Yam, V. W.-W. Phosphorescent Cyclometalated Platinum(II) Enantiomers with Circularly Polarized Luminescence Properties and Their Assembly Behaviors. *J. Am. Chem. Soc.* **2021**, *143*, 21676−21684.
(30) Tang, X.; Jiang, H.; Si, Y.; Rampal, N.; Gong, W.; Cheng, C.; Kang, X.; Fairen-Jimenez, D.; Cui, Y.; Liu, Y. Endohedral functionalization of chiral metal-organic cages for encapsulating achiral dyes to induce circularly polarized luminescence. *Chem* **2021**, *7*, 2771−2786.
(31) Kitagawa, Y.; Tsurui, M.; Hasegawa, Y. Steric and Electronic Control of Chiral Eu(III) Complexes for Effective Circularly Polarized Luminescence. *ACS Omega* **2020**, *5*, 3786−3791.

(32) Hu, S.-J.; Guo, X.-Q.; Zhou, L.-P.; Yan, D.-N.; Cheng, P.-M.; Cai, L.-X.; Li, X.-Z.; Sun, Q.-F. Guest-Driven Self-Assembly and Chiral Induction of Photofunctional Lanthanide Tetrahedral Cages. *J. Am. Chem. Soc.* **2022**, *144*, 4244−4253.
(33) Wu, K.; Tessarolo, J.; Baksi, A.; Clever, G. H. Guest-Modulated Circularly Polarized Luminescence by Ligand-to-Ligand Chirality Transfer in Heteroleptic PdII Coordination Cages. *Angew. Chem., Int. Ed.* **2022**, *61*, No. e202205725.
(34) Jiao, J.; Tan, C.; Li, Z.; Liu, Y.; Han, X.; Cui, Y. Design and Assembly of Chiral Coordination Cages for Asymmetric Sequential Reactions. *J. Am. Chem. Soc.* **2018**, *140*, 2251−2259.
(35) Schulte, T. R.; Holstein, J. J.; Clever, G. H. Chiral Self-Discrimination and Guest Recognition in Helicene-Based Coordination Cages. *Angew. Chem., Int. Ed.* **2019**, *58*, 5562−5566.
(36) Tateishi, T.; Kojima, T.; Hiraoka, S. Chiral self-sorting process in the self-assembly of homochiral coordination cages from axially chiral ligands. *Commun. Chem.* **2018**, *1*, 20.
(37) Grajda, M.; Staros, G.; Jędrzejewska, H.; Szumna, A. Toward Coordination Cages with Hybrid Chirality: Amino Acid-Induced Chirality on Metal Centers. *Inorg. Chem.* **2022**, *61*, 11410−11418.
(38) Wu, H.-B.; Wang, Q.-M. Construction of Heterometallic Cages with Tripodal Metalloligands. *Angew. Chem., Int. Ed.* **2009**, *48*, 7343−7345.
(39) Xue, W.; Ronson, T. K.; Lu, Z.; Nitschke, J. R. Solvent Drives Switching between Λ and Δ Metal Center Stereochemistry of M_8L_6 Cubic Cages. *J. Am. Chem. Soc.* **2022**, *144*, 6136−6142.
(40) Greenfield, J. L.; Evans, E. W.; Di Nuzzo, D.; Di Antonio, M.; Friend, R. H.; Nitschke, J. R. Unraveling Mechanisms of Chiral Induction in Double-Helical Metallopolymers. *J. Am. Chem. Soc.* **2018**, *140*, 10344−10353.
(41) Goswami, A.; Schmittel, M. Heteroleptic copper phenanthroline complexes in motion: From stand-alone devices to multicomponent machinery. *Coord. Chem. Rev.* **2018**, *376*, 478−505.
(42) Tan, Y. B.; Okayasu, Y.; Katao, S.; Nishikawa, Y.; Asanoma, F.; Yamada, M.; Yuasa, J.; Kawai, T. Visible Circularly Polarized Luminescence of Octanuclear Circular Eu(III) Helicate. *J. Am. Chem. Soc.* **2020**, *142*, 17653−17661.
(43) Wong, H.-Y.; Lo, W.-S.; Yim, K.-H.; Law, G.-L. Chirality and Chiroptics of Lanthanide Molecular and Supramolecular Assemblies. *Chem* **2019**, *5*, 3058−3095.
(44) Xuan, W.; Zhang, M.; Liu, Y.; Chen, Z.; Cui, Y. A Chiral Quadruple-Stranded Helicate Cage for Enantioselective Recognition and Separation. *J. Am. Chem. Soc.* **2012**, *134*, 6904−6907.
(45) Gütz, C.; Hovorka, R.; Struch, N.; Bunzen, J.; Meyer-Eppler, G.; Qu, Z. W.; Grimme, S.; Topic, F.; Rissanen, K.; Cetina, M.; Engeser, M.; Lutzen, A. Enantiomerically pure trinuclear helicates via diastereoselective self-assembly and characterization of their redox chemistry. *J. Am. Chem. Soc.* **2014**, *136*, 11830−11838.
(46) Shi, Q.; Zhou, X.; Yuan, W.; Su, X.; Neniškis, A.; Wei, X.; Taujenis, L.; Snarskis, G.; Ward, J. S.; Rissanen, K.; et al. Selective Formation of S4- and T-Symmetric Supramolecular Tetrahedral Cages and Helicates in Polar Media Assembled via Cooperative Action of Coordination and Hydrogen Bonds. *J. Am. Chem. Soc.* **2020**, *142*, 3658−3670.
(47) Miyake, H.; Tsukube, H. Coordination chemistry strategies for dynamic helicates: time-programmable chirality switching with labile and inert metal helicates. *Chem. Soc. Rev.* **2012**, *41*, 6977−6991.
(48) Regeni, I.; Chen, B.; Frank, M.; Baksi, A.; Holstein, J. J.; Clever, G. H. Coal-Tar Dye-based Coordination Cages and Helicates. *Angew. Chem., Int. Ed.* **2021**, *60*, 5673−5678.
(49) Nishioka, Y.; Yamaguchi, T.; Kawano, M.; Fujita, M. Asymmetric [2 + 2] Olefin Cross Photoaddition in a Self-Assembled Host with Remote Chiral Auxiliaries. *J. Am. Chem. Soc.* **2008**, *130*, 8160−8161.
(50) Kaminker, R.; de Hatten, X.; Lahav, M.; Lupo, F.; Gulino, A.; Evmenenko, G.; Dutta, P.; Browne, C.; Nitschke, J. R.; van der Boom, M. E. Assembly of Surface-Confined Homochiral Helicates: Chiral Discrimination of DOPA and Unidirectional Charge Transfer. *J. Am. Chem. Soc.* **2013**, *135*, 17052−17059.
(51) Wu, G.; Chen, Y.; Fang, S.; Tong, L.; Shen, L.; Ge, C.; Pan, Y.; Shi, X.; Li, H. A Self-Assembled Cage for Wide-Scope Chiral Recognition in Water. *Angew. Chem., Int. Ed.* **2021**, *60*, 16594−16599.
(52) Howlader, P.; Mondal, S.; Ahmed, S.; Mukherjee, P. S. Guest-Induced Enantioselective Self-Assembly of a Pd6 Homochiral Octahedral Cage with a C3-Symmetric Pyridyl Donor. *J. Am. Chem. Soc.* **2020**, *142*, 20968−20972.
(53) Ouyang, J.; Swartjes, A.; Geerts, M.; Gilissen, P. J.; Wang, D.; Teeuwen, P. C. P.; Tinnemans, P.; Vanthuyne, N.; Chentouf, S.; Rutjes, F. P. J. T.; et al. Absolute configuration and host-guest binding of chiral porphyrin-cages by a combined chiroptical and theoretical approach. *Nat. Commun.* **2020**, *11*, No. 4776.
(54) Cui, D.-X.; Geng, Y.; Kou, J.-N.; Shan, G.-G.; Sun, C.-Y.; Zhang, K.-H.; Wang, X.-L.; Su, Z.-M. Chiral self-sorting and guest recognition of porous aromatic cages. *Nat. Commun.* **2022**, *13*, No. 4011.
(55) Hu, Q.-P.; Zhou, H.; Huang, T.-Y.; Ao, Y.-F.; Wang, D.-X.; Wang, Q.-Q. Chirality Gearing in an Achiral Cage through Adaptive Binding. *J. Am. Chem. Soc.* **2022**, *144*, 6180−6184.
(56) Li, B.; Zheng, B.; Zhang, W.; Zhang, D.; Yang, X.-J.; Wu, B. Site-selective binding of peripheral chiral guests induces stereospecificity in A_4L_6 tetrahedral anion cages. *J. Am. Chem. Soc.* **2020**, *142*, 6304−6311.
(57) Schmidt, A.; Casini, A.; Kühn, F. E. Self-assembled M_2L_4 coordination cages: Synthesis and potential applications. *Coord. Chem. Rev.* **2014**, *275*, 19−36.
(58) De, S.; Mahata, K.; Schmittel, M. Metal-coordination-driven dynamic heteroleptic architectures. *Chem. Soc. Rev.* **2010**, *39*, 1555−1575.
(59) Akine, S.; Miyake, H. Stimuli-responsive chirality inversion of metallohelices and related dynamic metal complexes. *Coord. Chem. Rev.* **2022**, *468*, No. 214582.
(60) Hutin, M.; Bernardinelli, G.; Nitschke, J. R. Synthetic selectivity through avoidance of valence frustration. *Proc. Natl. Acad. Sci. U.S.A.* **2006**, *103*, 17655−17660.
(61) Ruben, M.; Rojo, J.; Romero-Salguero, F. J.; Uppadine, L. H.; Lehn, J.-M. Grid-Type Metal Ion Architectures: Functional Metallosupramolecular Arrays. *Angew. Chem., Int. Ed.* **2004**, *43*, 3644−3662.
(62) Zhang, Q.; Komino, T.; Huang, S.; Matsunami, S.; Goushi, K.; Adachi, C. Triplet Exciton Confinement in Green Organic Light-Emitting Diodes Containing Luminescent Charge-Transfer Cu(I) Complexes. *Adv. Funct. Mater.* **2012**, *22*, 2327−2336.
(63) Greenfield, J. L.; Di Nuzzo, D.; Evans, E. W.; Senanayak, S. P.; Schott, S.; Deacon, J. T.; Peugeot, A.; Myers, W. K.; Sirringhaus, H.; Friend, R. H.; Nitschke, J. R. Electrically Induced Mixed Valence Increases the Conductivity of Copper Helical Metallopolymers. *Adv. Mater.* **2021**, *33*, No. 2100403.
(64) Fujita, M.; Nagao, S.; Ogura, K. Guest-Induced Organization of a Three-Dimensional Palladium(II) Cagelike Complex. A Prototype for "Induced-Fit" Molecular Recognition. *J. Am. Chem. Soc.* **1995**, *117*, 1649−1650.
(65) Domoto, Y.; Abe, M.; Fujita, M. A Highly Entangled $(M_3L_2)_8$ Truncated Cube from the Anion-Controlled Oligomerization of a π-Coordinated M_3L_2 Subunit. *J. Am. Chem. Soc.* **2021**, *143*, 8578−8582.
(66) Vilar, R. Anion Recognition and Templation in Coordination Chemistry. *Eur. J. Inorg. Chem.* **2008**, *2008*, 357−367.
(67) Gao, W.-X.; Feng, H.-J.; Guo, B.-B.; Lu, Y.; Jin, G.-X. Coordination-Directed Construction of Molecular Links. *Chem. Rev.* **2020**, *120*, 6288−6325.
(68) Hutin, M.; Cramer, C. J.; Gagliardi, L.; Shahi, A. R. M.; Bernardinelli, G.; Cerny, R.; Nitschke, J. R. Self-sorting chiral subcomponent rearrangement during crystallization. *J. Am. Chem. Soc.* **2007**, *129*, 8774−8780.
(69) Maglic, J. B.; Lavendomme, R. MoloVol: an easy-to-use program for analyzing cavities, volumes and surface areas of chemical structures. *J. Appl. Crystallogr.* **2022**, *55*, 1033−1044.
(70) Kang, S. O.; Begum, R. A.; Bowman-James, K. Amide-Based Ligands for Anion Coordination. *Angew. Chem., Int. Ed.* **2006**, *45*, 7882−7894.

https://doi.org/10.1021/jacs.3c11321
J. Am. Chem. Soc. 2024, 146, 2379−2386

(71) Custelcean, R. Anion encapsulation and dynamics in self-assembled coordination cages. *Chem. Soc. Rev.* **2014**, *43*, 1813−1824.
(72) Harrison, E. E.; Waters, M. L. Detection and Differentiation of Per- and Polyfluoroalkyl Substances (PFAS) in Water Using a Fluorescent Imprint-and-Report Sensor Array. *Chem. Sci.* **2023**, *14*, 928−936.
(73) Sakata, Y.; Chiba, S.; Akine, S. Transient chirality inversion during racemization of a helical cobalt(III) complex. *Proc. Natl. Acad. Sci. U.S.A.* **2022**, *119*, No. e2113237119.
(74) Sun, B.; Nurttila, S. S.; Reek, J. N. H. Synthesis and Characterization of Self-Assembled Chiral $Fe^{II}_2L_3$ Cages. *Chem. − Eur. J.* **2018**, *24*, 14693−14700.
(75) Luo, D.; Yuan, Z.-J.; Ping, L.-J.; Zhu, X.-W.; Zheng, J.; Zhou, C.-W.; Zhou, X.-C.; Zhou, X.-P.; Li, D. Tailor-Made Pd_nL_{2n} Metal-Organic Cages through Covalent Post-Synthetic Modification. *Angew. Chem., Int. Ed.* **2023**, *62*, No. e202216977.
(76) Wu, K.; Li, K.; Hou, Y.-J.; Pan, M.; Zhang, L.-Y.; Chen, L.; Su, C.-Y. Homochiral D_4-symmetric metal−organic cages from stereogenic Ru(II) metalloligands for effective enantioseparation of atropisomeric molecules. *Nat. Commun.* **2016**, *7*, No. 10487.
(77) Terpin, A. J.; Ziegler, M.; Johnson, D. W.; Raymond, K. N. Resolution and Kinetic Stability of a Chiral Supramolecular Assembly Made of Labile Components. *Angew. Chem., Int. Ed.* **2001**, *40*, 157−160.
(78) Ikeda, A.; Udzu, H.; Zhong, Z.; Shinkai, S.; Sakamoto, S.; Yamaguchi, K. A Self-Assembled Homooxacalix[3]arene-based Dimeric Capsule Constructed by a Pd^{II}−Pyridine Interaction Which Shows a Novel Chiral Twisting Motion in Response to Guest Inclusion. *J. Am. Chem. Soc.* **2001**, *123*, 3872−3877.
(79) Wan, S.; Lin, L.-R.; Zeng, L.; Lin, Y.; Zhang, H. Efficient optical resolution of water-soluble self-assembled tetrahedral M_4L_6 cages with 1,1′-bi-2-naphthol. *Chem. Commun.* **2014**, *50*, 15301−15304.
(80) Castilla, A. M.; Ousaka, N.; Bilbeisi, R. A.; Valeri, E.; Ronson, T. K.; Nitschke, J. R. High-Fidelity Stereochemical Memory in a $Fe^{II}_4L_4$ Tetrahedral Capsule. *J. Am. Chem. Soc.* **2013**, *135*, 17999−18006.
(81) Mara, M. W.; Fransted, K. A.; Chen, L. X. Interplays of excited state structures and dynamics in copper(I) diimine complexes: Implications and perspectives. *Coord. Chem. Rev.* **2015**, *282*−*283*, 2−18.

https://doi.org/10.1021/jacs.3c11321
J. Am. Chem. Soc. 2024, 146, 2379−2386